Neurobiology of Disease

Long-Term Changes in Trigeminal Ganglionic and Thalamic Neuronal Activities following Inferior Alveolar Nerve Transection in Behaving Rats

Wan-Ting Tseng,[1] Meng-Li Tsai,[2] Koichi Iwata,[3] and Chen-Tung Yen[1,4]

[1]Institute of Zoology, National Taiwan University, Taipei, 106 Taiwan; [2]Department of Biomechatronic Engineering, National Ilan University, Ilan, 260 Taiwan; [3]Department of Physiology, School of Dentistry, Nihon University, 101-8310 Tokyo, Japan; and [4]Neurobiology and Cognitive Science Center, National Taiwan University, 106 Taiwan

The transection of the inferior alveolar nerve (IANx) produces allodynia in the whisker pad (V2 division) of rats. Ectopic discharges from injured trigeminal ganglion (TG) neurons and thalamocortical reorganization are possible contributors to the sensitization of uninjured V2 primary and CNS neurons. To test which factor is more important, TG and ventroposterior medial nucleus (VPM) neurons were longitudinally followed before, during, and after IANx for up to 80 d. Spontaneous discharges and mechanical stimulation-evoked responses were recorded in conscious and in anesthetized states. Results show (1) a sequential increase in spontaneous activities, first in the injured TG neurons of the IAN (2–30 d), followed by uninjured V2 ganglion neurons (6–30 d), and then VPM V2 neurons (7–30 d) after IANx; (2) ectopic discharges included burst and regular firing patterns in the IAN and V2 branches of the TG neurons; and (3) the receptive field expanded, the modality shifted, and long-lasting after-discharges occurred only in VPM V2 neurons. All of these changes appeared in the late or maintenance phase (7–30 d) and disappeared during the recovery phase (40–60 d). These observations suggest that ectopic barrages in the injured IAN contribute more to the development of sensitization, whereas the modality shift and evoked after-discharges in the VPM thalamic neurons contribute more to the maintenance phase of allodynia by redirecting tactile information to the cortex as nociceptive.

Introduction

Peripheral nerve injury often causes chronic neuropathic pain, which is the clinical condition in which persistent pain arises either spontaneously or after light touch (allodynia) on the skin (Woolf and Mannion, 1999). Animal studies have suggested that the early onset of ectopic discharges of the primary afferent neurons at 4–8 h after nerve injury (Sun et al., 2005) may be involved in the development of neuropathic pain (Ji and Strichartz, 2004; Devor, 2009a).

However, these ectopic discharge observations were obtained in acute electrophysiological studies. Injury discharges, which mimic ectopic discharges, may result from nerve stretching, dehydration, decreased calcium levels of damaged nerves (Wall et al., 1974), and electrode penetration (Macefield, 1998) in acute recording experiments. We recently developed a chronic, multichannel single-unit recording method (Tseng et al., 2011) for implanting a microwire electrode in the trigeminal ganglion (TG). The first objective of this study is to monitor TG neuronal activity changes longitudinally before, during, and after inferior alveolar nerve transection (IANx).

The proposed technique has the advantage of recording neural activity under waking conditions. To clarify the mechanisms that cause neuropathic pain after peripheral nerve injury, many researchers have used general anesthesia to investigate the changes in neuronal excitability (for reviews, see Fried et al., 2001; Iwata et al., 2004; Takeda et al., 2011). However, this approach greatly suppresses neuronal activity (Kubota et al., 2007; Shoda et al., 2009) and makes it difficult to identify the exact mechanisms underlying pathological pain. Hence, it is important to compare the neuronal activity of rats with trigeminal neuropathic pain under the anesthetized and awake condition.

The lateral thalamus plays an important role in sensory gating, and may be involved in neuropathic pain following peripheral nerve injury (Vos et al., 2000; Hains et al., 2006; Jhaveri et al., 2008; Fischer et al., 2009). The rhythmic burst firing of thalamic neurons after peripheral nerve injury may contribute to the development of chronic pain (Lenz et al., 1989, 1994; Hains et al., 2006). Central sensitization may result from the enhanced activity of the primary afferent nerves after nerve injury (Campbell and Meyer, 2006; Costigan et al., 2009; Davis et al., 2011). Conversely, previous studies have shown that neuroplastic changes in the thalamocortical circuitry occurs within 3 h after nerve injury (Brüggemann et al., 2001; Komagata et al., 2011), indicating that

Received April 13, 2012; revised Aug. 31, 2012; accepted Sept. 17, 2012.

Author contributions: M.-L.T., K.I., and C.-T.Y. designed research; W.-T.T. performed research; W.-T.T. and M.-L.T. contributed unpublished reagents/analytic tools; W.-T.T. analyzed data; W.-T.T., K.I., and C.-T.Y. wrote the paper.

This work was supported by grants from the National Science Council, Taiwan (NSC100-2311-B002-002-MY3 and 100-2321-B-002-079) and one from the National Health Research Institutes, Taiwan (NHRI-EX101-10104NI).

Correspondence should be addressed to Dr. Chen-Tung Yen, Institute of Zoology, National Taiwan University, 1 Roosevelt Road, Sec. 4, Taipei, 106, Taiwan. E-mail: ctyen@ntu.edu.tw.

DOI:10.1523/JNEUROSCI.1828-12.2012

 0270-6474/12/3216051-13$15.00/0

central sensitization may also be involved in the development of neuropathic pain.

Therefore, the second objective of this study is to compare the changes in the excitability of neurons in the ventroposterior medial nucleus (VPM) of the thalamus versus those in the TG throughout the symptomatic period of IANx rats. This study reports results on the longitudinal changes of primary afferent and thalamic single-unit activities in conscious rats with peripheral nerve injury.

Materials and Methods

Adult female Sprague Dawley rats (290 ± 9 g) were used in this study. The rectal temperature of each anesthetized rat was monitored and maintained at 37°C using a feedback-controlled heating pad. All animal care and experimental procedures were approved by the Institutional Animal Care and Use Committee of National Taiwan University. The procedures adopted in this study were in accordance with the guidelines of the International Association for the Study of Pain (Zimmermann, 1983) and the "Codes for Experimental Use of Animals" of the Council of Agriculture of Taiwan, which is based on the Animal Protection Law of Taiwan.

Surgery for implantation. Mechanical hypersensitivity was tested with a modified von Frey test in which each rat would withdraw its nostril back into a dark box when its face was poked with the von Frey filament (Tsuboi et al., 2004). The rats were trained to withstand a force of 60 g. After successful behavior training, electrode sets were implanted into the TG and VPM, with one for each site. Full details of how to fabricate the bundled microarray electrode sets and surgical implant procedures have been reported previously (Tseng et al., 2011). Briefly, rats were anesthetized with sodium pentobarbital (50 mg/kg, i.p.). Supplemental doses (16 mg/kg, i.p.) of the same anesthetic were administered when necessary. Craniotomies were performed to expose the brain surface vertical to the recording sites within the TG (left, 2.5–3.5 mm; posterior 5.5–6.5 mm to bregma) and VPM (right, 2–3 mm; posterior 3.5–4.5 mm to bregma). The bundled electrode set for the TG consisted of three or four tungsten microwires (with diameters of 35 μm bare and 50 μm insulated (#100211; California Fine Wire) in a 30-G guide tube. The electrode bundle was inserted perpendicularly and located at a depth of 9.5 mm, where single-unit activity responsiveness to tactile stimulation of the ipsilateral face could be identified in at least two microwires. The electrode set for the thalamus consisted of seven tungsten microwires in a 29-G guide tube and aimed for the contralateral VPM at a depth of 5 to 6– mm, where single-unit activity responsiveness to tactile stimulation of the ipsilateral face could be detected in at least 4 microwires.

Four stainless steel screws were set in the skull to serve as anchors for the electrode sets. For electroencephalogram (EEG) recording, a bare copper wire was wound around one of the anchoring screws, which was placed 1 mm posterior to the bregma and 1 mm lateral to the midline. Two flexible stainless steel wires (7-stranded, #793200; AM System) were implanted in the neck muscles, one in each side, to record electromyogram (EMG) data. When all the electrodes were in place, the surface of the skull was covered with dental cement, and the wound was sutured. Lincomycin hydrochloride (30 mg/kg, i.m.) was administrated to prevent infection. The rats were allowed to recuperate from possible brain and ganglia damage in the implanting process for at least 14 d (Tseng et al., 2011).

Behavioral test. The behavioral test in this study followed a method described by Tsuboi et al. (2004). Testing was conducted during the daytime (9:00 A.M. to 5:00 P.M.). In daily sessions, rats were trained to remain stable in a carton (13 × 7 × 8 cm) with their snouts protruding through a hole (2 cm in diameter) in the wall during mechanical stimulation of the left and right whisker pads with a series of nine von Frey filaments (1, 2, 4, 6, 8, 10, 15, 26, and 60 g; Touch-Test, North Coast Medical). Beginning with the lowest intensity, quantitative mechanical stimuli were applied in an ascending-descending-ascending order to evaluate the median escape threshold. Each von Frey filament was applied to the whisker pad 10 times at 1 Hz. When rats showed a brisk withdrawal response, the intensity of that filament was defined as the first escape threshold. The filaments were sequentially applied in descending order to determine the strongest filament for which the rats would not escape for all 10 trials, and this filament intensity was recorded as the second escape threshold. The same ascending procedure used to define the first escape threshold was used to determine the third escape threshold. The median escape threshold was determined from these three escape threshold values.

The criterion performance was when rats could withstand a 60 g mechanical stimulus on their whisker pad without exhibiting any escape behavior. Electrode-implantation surgery was performed the day after the rat achieved the criterion performance. The threshold for escape from mechanical stimulation of the whisker pad was then measured 3, 6, 10, 13, and 17 d after implantation to ensure that inflammation induced by the implant surgery had disappeared. IAN injury was produced at least 2 weeks after implantation (Tseng et al., 2011). The escape threshold was then determined on 1, 3, 7, 14, 20, 30, 40, 50, and 60 d after IANx.

IANx. When implanted rats could withstand a 60 g von Frey filament stimulation, IANx was performed the next day after a baseline electrophysiological recording (see below) under mask anesthesia (2–3% isoflurane-O_2 mixture). The neuronal activities of the TG and VPM were recorded during the IANx procedure (Iwata et al., 2001) to monitor and record any abnormal discharges. A small incision was made on the surface of the left facial skin and masseter muscle. Removing the covering alveolar bone exposed the IAN and mental nerves. These nerves were then transected followed by tight ligation with 6-0 silk at two points on the nerve trunk with an interpoint gap size of 1 mm. For sham-operated rats, the facial skin and muscle were incised, and the surface of the alveolar bone was removed. Care was taken not to touch the nerves. After surgery, lincomycin hydrochloride (30 mg/kg, i.m.) was administrated to prevent infection.

Electrophysiological recording. Longitudinal neuronal activities in the same rat were monitored and recorded during IANx, from 1 to 6 h after IANx, and 1, 2, 3, 7, 14, 20, 30, 40, 50, and 60 d after IANx. In each daily session (before and on the days after IANx), rats were placed in a plastic transparent chamber (20 × 14 × 35 cm) with a mirror in the back of the chamber. A video camera was placed 1.6 m in front of the chamber. Spikes and EEG and EMG activities were transmitted through a connecting cable to a multichannel acquisition processor system (MAP; Plexon). After acclimatization, the rat's spontaneous behaviors were sampled (CinePlex; Plexon) at 30 frames per second and synchronized with the neuronal recording for 10 min. For single-unit recordings, spikes were amplified (7000- to 32,000-fold), filtered (0.25–kHz), and digitized at 40 kHz. EEG and EMG activity signals were amplified (5000- to 10,000-fold), filtered (0.7–170 Hz), and digitized at 1 kHz. Extracellular single units were recorded in real time using time-voltage windows and a principle component-based template-matching algorithm (Sort Client; Plexon). Another data acquisition system (Model ML870; PowerLab 8/30) simultaneously recorded selected highpass-filtered raw signals at a rate of 20 kHz per channel using PowerLab software (version 5; ADInstruments) to capture and analyze continuous signals.

The rat was then removed from the testing room and anesthetized with continuous inhalation of a 1% isoflurane-O_2 mixture. After quantifying the receptive field (RF), spontaneous activities were recorded for 10 min under anesthesia. The evoked responses to mechanical stimuli of the RF were then recorded. General mechanical stimulations consisted of hair stimulation with a puff of air, cutaneous stimulation with a gentle brush, and noxious stimulation with a rodent pincher (RP-1; BIOSEB) on a 20 mm^2 stimulus area. Additional mechanical stimulations were applied as follows: (1) von Frey filaments (1, 6, 15, 26, and 60 g), (2) a handheld fine stick used to stimulate individual guard hairs and whiskers, and (3) a cotton swab used to stimulate a tooth with a scratching movement. Each stimulation was applied for 5–10 s, and the minimum interstimulus interval (ISI) was set to 30 s. The border of the RF was determined under an operating microscope using the minimum intensity of stimulation.

IANx surgery was performed after recording baseline neuronal activity under conscious and anesthetized conditions. The recording began during the surgery immediately after IAN exposure and continued until the wound was sutured to identify any altered neuronal discharges immediately after nerve injury. Isoflurane anesthesia was discontinued and the

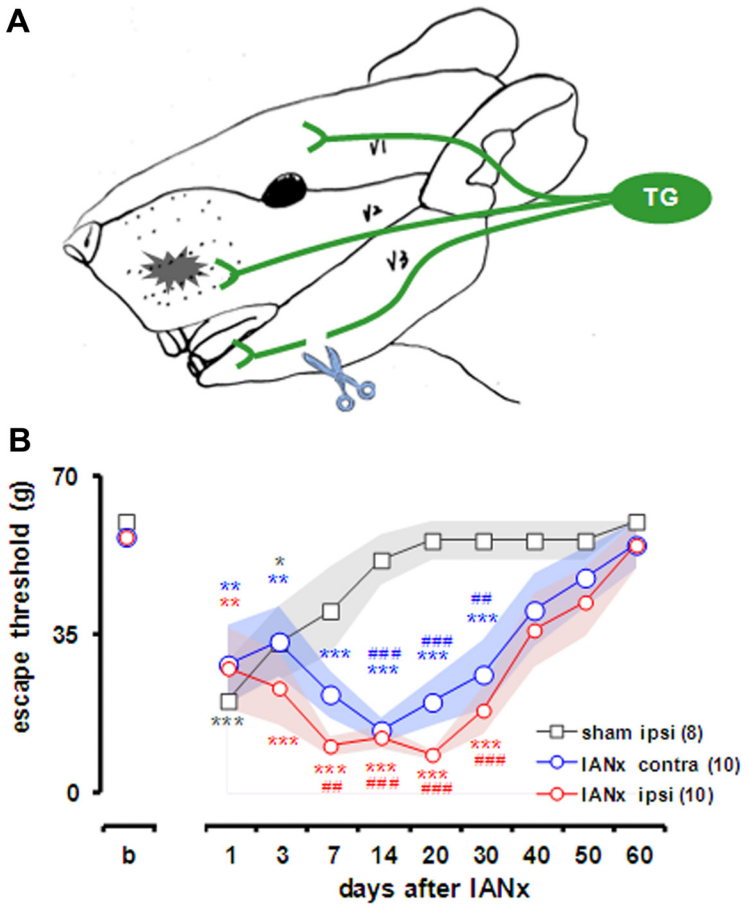

Figure 1. Diagram of IANx model and tactile allodynia. ***A***, IAN, a branch of V3 division of trigeminal nerve, is cut and the skin of whisker pad (V2 division) is sensitized (black, spiky spot). ***B***, Face-escape threshold to von Frey stimuli before (b) and 1–60 d after IANx or a sham operation. Repeated-measures ANOVA showed significant differences between IANx ipsilateral/IANx contralateral and sham-operated ipsilateral groups indicated by $^{\#\#}p < 0.01$ and $^{\#\#\#}p < 0.001$; significant decreases on both sides of the face 1–30 d after IANx: $^{*}p < 0.05$, $^{**}p < 0.01$, and $^{***}p < 0.001$ (compared with the value before IANx). Shaded areas denote the mean ± SEM. Numerals in parentheses are the numbers of rats. ipsi, ipsilateral side to IANx; contra, contralateral side to IANx; b, before the operation.

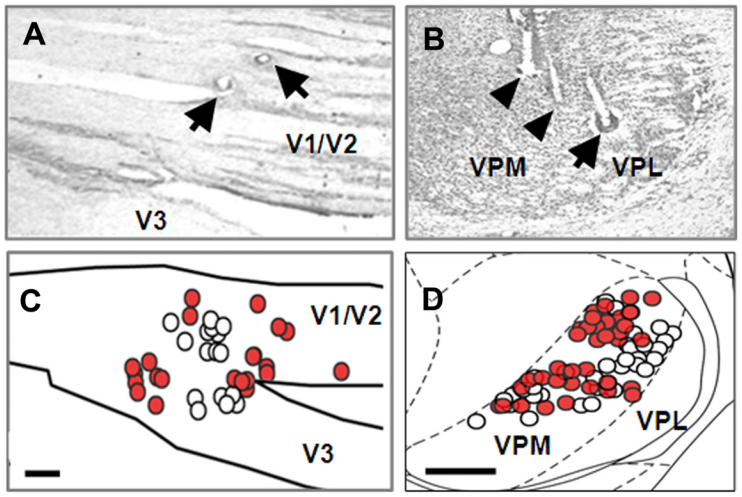

Figure 2. Recording sites. ***A***, ***B***, Examples of histological sections of the TG and thalamus. Locations of successful recording were determined by electrolytic lesions (arrows). All TG (***C***) and VPM (***D***). Summary of locations of unit recorded from IANx (red circle) and sham-operated (open circle) rats. Arrowheads, tracks of microwires; V1 to V3, first to third branches of the trigeminal nerve. Scale bars: 500 μm.

rat was placed in a transparent observation chamber. The rat recovered from the isoflurane anesthesia 1 h after IANx and could walk around the chamber. Spontaneous neuronal and behavior recordings in the conscious condition were taken for 10 min once every hour for 6 h after IANx. Rats were not anesthetized a second time during this 6 h period. From the second day after IANx and afterward, daily measurements included the head-withdrawal behavioral test, resting wakeful electrophysiological recording, and resting and stimulated electrophysiological recording under isoflurane anesthesia.

Histology. After taking all recordings, rats were anesthetized with sodium pentobarbital (60 mg/kg), and electrolytic lesions (30 μA for 10 s, three times) were made at selected sites. The rats were perfused intracardially with saline followed by a 10% formalin solution. The brain and TG were removed and postfixed in the same fixative. Tissues were transferred to 20% sucrose in a 0.1 M phosphate buffer 2 d before frozen sectioning. The tissues were frozen-sectioned into 50 μm slices and processed with Nissl staining. Implantation tracts and lesion sites were identified and recorded with a Zeiss Axioplan 2 microscope (Carl Zeiss) connected to a Nikon digital camera.

Data analysis. Spike waveforms were saved and re-sorted using Offline Sorter (Plexon), which is based on principle component clustering, with a user-defined template. The same template was applied to all waveform data from all recording days of the same channel in each animal. The unit identity across multiple days was defined by similar waveform shapes and RFs. After IANx, many V3 units lost their RF. Thus, the stability of these units could only be evaluated by waveform similarity. According to these criteria, ~2 units per microwire channel were isolated throughout the 60 d recording period. Our previous study (Tseng et al., 2011) presents the details of linear correlations between waveforms and the principle component stability tube (PCST) used to evaluate the stability of the unit recording.

Epochs of resting behavior were extracted from 10 min data using CinePlex software with the following definitions: (1) the rat was relaxed with both eyes open, and without movement, as confirmed by the small amplitude of EMG data; (2) the left side of the rat's face (RF of the units) was not in contact with anything; and (3) there was a low amplitude of the EEG. For each epoch, the spike numbers of each unit were divided by the epoch duration. Spontaneous activity during conscious resting was then represented as the mean firing frequency of these resting epochs.

Spontaneous activity under anesthesia was presented as the mean value of 10 min data. Evoked responses to mechanical stimulation of each unit were calculated by the mean value during the stimulation subtracted by the average baseline activity in the 10 s period before the stimulation. The units were determined to be responsive if three continuous bins (with a bin size of 1 s) of the histogram during the

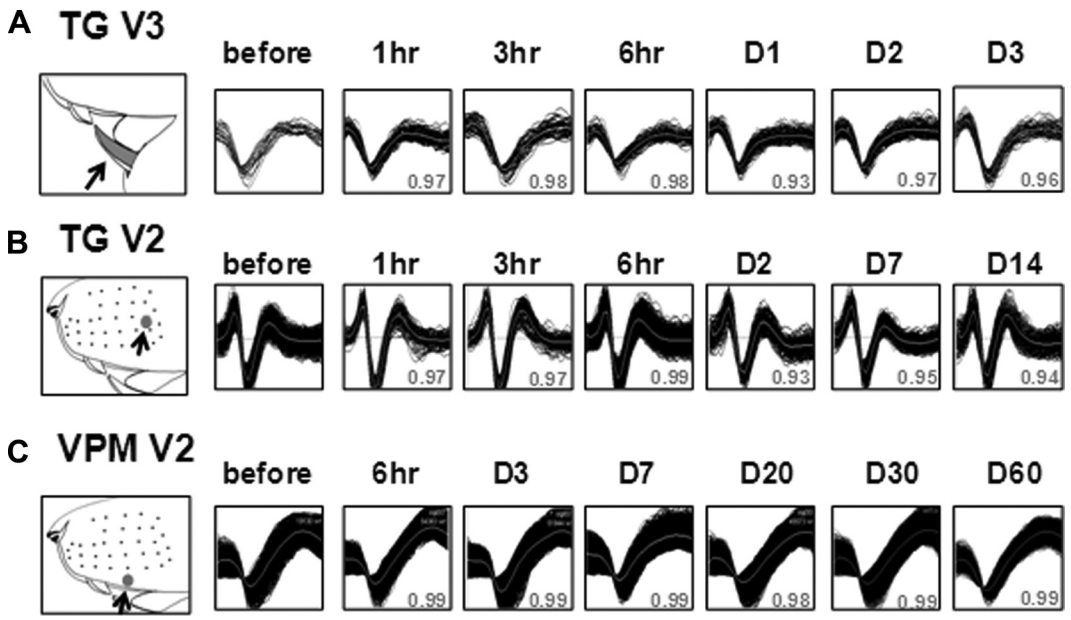

Figure 3. Representative waveforms of stable TG (***A***, ***B***) and VPM (***C***) units from the same microwire across days. All waveforms during the 10 min recording period on each recording session are shown. The RF of each unit is shown on the left. Stability was quantified by the maximum *r* value (gray numeral below each waveform), by comparing the average waveform of a given recording session with the one before IANx.

stimulus exceeded the threshold, calculated as the mean + 2.33 SDs of the 10 s data before each stimulus. A "low-threshold unit" was defined as a unit that only responded to innocuous stimulations, and a "nociceptive unit" was defined as a unit that responded to noxious stimulation. All of the values were analyzed using NeuroExplorer (Nex Technologies) and MATLAB software (MathWorks). The spontaneous activity of VPM V2 units and the tactile-evoked response of the TG V2 units and VPM V2 units were normalized and divided by the average discharge rate of the TG V2 units and VPM V2 units in the sham-operated group.

The statistical analysis in this study included a two-way repeated-measures ANOVA followed by the Tukey's *post hoc* test for the behavioral test. The Mann–Whitney *U* test was used to test the differences in firing rates of spontaneous activities, evoked responses, and RF sizes between the IANx and sham-operated groups, and between paired groups (before and after IANx). Kruskal–Wallis ANOVA with Dunn's *post hoc* method was used for comparing onset time of TG IAN, TG V2, and VPM V2. Comparisons of spontaneous activity between the awake and anesthetized conditions and modality shifts were computed using a paired *t* test or Wilcoxon signed-rank test. χ^2 or Fisher's exact test was used to evaluate differences in the occurrence rate of the modality shift between the IANx and sham-operated groups. This study presents results as the mean ± SEM and considers differences to be significant at $p < 0.05$.

Results

In IANx rats ($n = 10$), both sides of their faces began to exhibit significant mechanical allodynia 1 d after nerve transection, and this condition persisted to day 30 (Fig. 1). Although sham-operated rats ($n = 8$) also developed allodynia immediately after the operation, they recovered after 3 d. According to the pattern of behavioral changes, IANx neuropathic allodynia was separated into three phases: early (or development phase, 0–3 d), late (or maintenance phase, 7–d), and recovery (40–60 d) phases.

Chronic recordings were taken in 77 TG and 163 VPM units. However, only V2 and V3 units that could be recorded for >2 sessions were further analyzed. Based on these criteria, 156 units were selected for further analysis. During chronic longitudinal recording, many new units emerged after IANx or sham surgery (new units) in addition to the units that were recorded in the presurgery baseline condition (pre-existing unit). Only new units with V2 and V3 RFs were included, with the exception of V3 units emerging from the IAN unit recording microwires after IAN transection. In this case, no RF could be identified. Figure 2 shows the recording sites of the units identified by lesion marks.

Sixty-four stable units in TG (45 in IANx and 19 in sham-operated rats) and 92 in VPM (46 in IANx and 46 in sham-operated rats) had similar waveforms and RFs across at least two recording sessions. The stability of these units across the recording sessions was quantified by examining the similarity of the waveforms (see Materials and Methods) and RFs. Figure 3 shows examples of the waveforms of stable units across days. The average correlation coefficients of the waveform pairs of the TG and VPM were 0.980 ± 0.003 and 0.980 ± 0.002, respectively. Pre-existing units were used to analyze changes the RF, and the modality shift. New units that emerged after the IANx/sham operation were pooled with pre-existing units to analyze spontaneous activity, firing patterns, and tactile-evoked responses.

Injury discharges after transection under anesthesia

It was reported that the injured fibers exhibited prolonged injury discharges at >20 Hz after sectioning, which lasted ~30 min (Adrian, 1930; Chung et al., 1992). These impulses are likely the trigger of neuropathic pain behavior (Seltzer et al., 1991). Unit activity was continuously recorded during surgery to test whether injured fibers generated prolonged injury discharges after IANx. Results show that 2 of the 11 pre-existing TG V3 units exhibited prolonged slow-rate discharges (<0.05 Hz) immediately after nerve cutting. At 30 min after sectioning, these two units became silent and one of them reactivated (0.35 Hz) at 5 h after IANx. Another nine pre-existing TG V3 units displayed brief impulses after transection, and then became silent.

Because the IANx procedure involves tying and removing a piece of IAN nerve, silencing of the TG fiber might be due to a loss of recording caused by the position change of the V3 TG branch in the ganglion. To identify whether the silent TG V3 units were not lost, a pilot experiment was performed using preimplanted TG recording and electrical stimulation of the transected nerve.

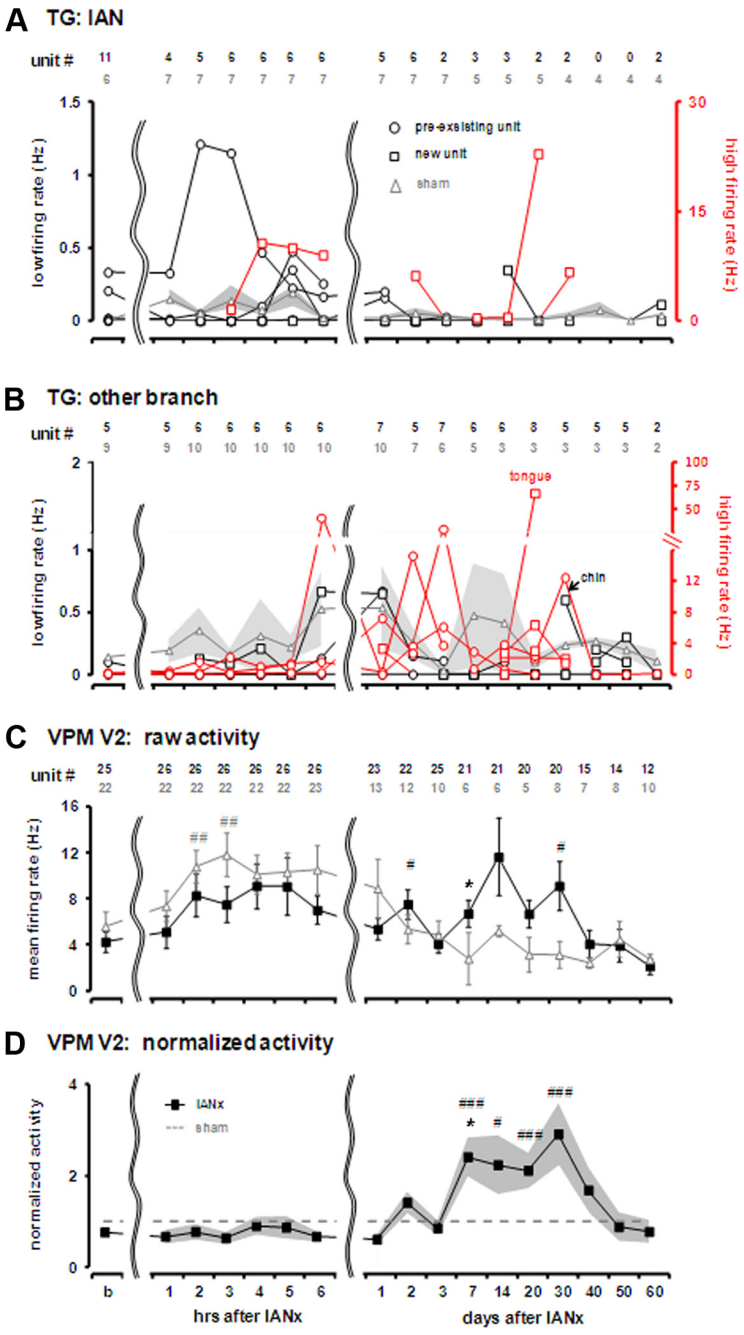

Figure 4. Sequential initiation of abnormal spontaneous firing in TG primary afferents and VPM in awake rats. ***A***, Spontaneous ectopic activity of TG V3 units of the transected IAN, including new units without an RF, which began at the same day of the lesion. The right side of the *y*-axis is for units with high spontaneous activities (red), and the left side is for slower activities (black). Value of the unit discharge of the sham-operated group is presented as the mean ± SEM in the shaded area. ***B***, Spontaneous activity of all TG V2 units plus two TG V3 units from uninjured nerve branches. RFs of these two TG V3 units were, respectively, in the tongue and chin. Increased spontaneous activities were mostly recorded on the second day and in the early and late stages. ***C***, Raw VPM spontaneous activity in IANx and sham rats. Numerals listed at the top of each part are the unit number at each recording session in the transection of the IAN (IANx; black) and sham-operated (gray) rats. ***D***, Normalized VPM spontaneous activity, divided by the average discharge rate of those in the sham-operated group. $^{\#}p < 0.05$, $^{\#\#}p < 0.01$, $^{\#\#\#}p < 0.001$ versus baseline (before IANx, b). $^{*}p < 0.05$, versus the sham-operated group (original firing rates of the IANx and sham-operated groups were compared).

Large spontaneous activity was observed in TG V3 units immediately after IANx, and these units became silent 30 min thereafter. A coaxial stimulus electrode was placed on the proximal end of the IAN, and an electrical current (300 μA, 0.01 ms) was repeatedly delivered at 0.5 Hz. This electrical stimulation activated action potentials with the same waveform as those before transection. These results confirm that pre-existing TG V3 units were silent, but not lost, after transection.

Time course in the change of spontaneous TG and VPM activity in conscious rats

In intact rats (before IANx), all pre-existing TG units had slow, spontaneous neuronal activity (TG V3: 0.05 ± 0.03 Hz, TG V2: 0.10 ± 0.03 Hz) in the resting conscious condition. They had higher firing rates after nerve injury. The initiation of abnormal firing in injured TG V3 units occurred earlier than other uninjured branches of the trigeminal nerve (Fig. 4*A*). Four of the 11 pre-existing TG V3 units (i.e., 36%) became activated 2–4 h after IANx, whereas the others remained silent. Among the new IAN units emerging after IANx, 40% (6 of 15) exhibited fast, spontaneous activity in the early (3 h) and late phases of allodynia.

In sham-operated rats, none of the six pre-existing and stable TG V3 units showed a marked increase in spontaneous activity after the operation (Fig. 4*A*).

Delayed activation of TG V2 units began 6 h after IANx and lasted 30 d (Fig. 4*B*). Sixty percent of pre-existing units (3 of 5 units) and 43% of new units (6 of 14 units) were activated. In contrast, none of the nine pre-existing and stable TG V2 units changed their spontaneous activity after the sham operation (Fig. 4*B*). Two TG V3 units, emerging at 14 and 30 d, respectively, had RFs located in the tongue and under the chin (not in the innervation territory of the IAN). These units showed increased spontaneous activity in the late maintenance phase at 20 and 30 d, respectively (Fig. 4*B*).

High-frequency firing in VPM V2 units was observed 7 d after transection, and this firing continued until 30 d (Fig. 4*D*). The onset of high-frequency firing (> mean + 2 SD of baseline) was significantly later in VPM V2 units (14.20 ± 2.35 d, 27 of 46 units) than TG V3 units (0.61 ± 0.40 d, 10 of 26 units), according to Kruskal–Wallis ANOVA with Dunn's *post hoc* method ($p < 0.05$). There was no significant difference of onset between TG V2 units (9.66 ± 4.90 d, 9 of 19 units) and TG V3 units, and between VPM V2 units and TG V2 units. In contrast, during the same period (7–30 d), the VPM V2 units in sham-operated rats ($n = 46$) did not show higher spontaneous activity (Fig. 4*C*).

Rapid thalamic sensitization (2–5 h after IANx) occurred in IANx rats and sham rats (Fig. 4*C*). During this period (2–5 h after operation), the original spontaneous activity of the VPM V2 units in both IANx (8.47 ± 1.63 Hz, 26 units) and sham-operated rats

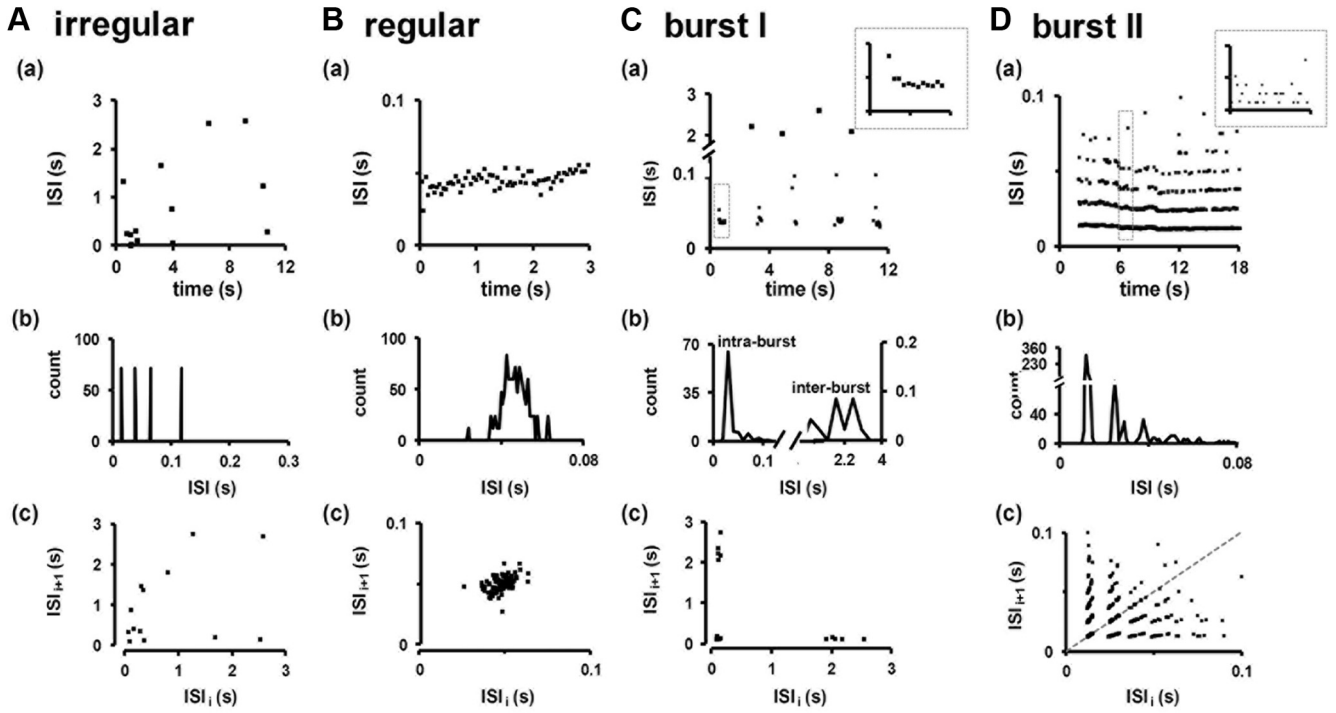

Figure 5. Ectopic firing pattern of the TG in awake rats with IANx. The ISI distribution of slow irregular (***A***), regular (***B***), burst I (***C***), and burst II (***D***) firing. ***Aa–Da***, Representative examples of ISI versus time plots for four types of firing pattern. Each point indicates a single interval between two consecutive spikes. The *y*-axis in ***Ca*** is adjusted to emphasize the ISIs of <0.1 s. Detailed ISI distributions to the dashed gray box in ***Ca*** and ***Da*** are shown in the insets. ISI histogram and ISI return map of data in (***a***) display, respectively, in (***b***) and (***c***). ***Cb***, Burst I shows two main peaks, indicating the ISI of intrabursts (short, 40 ms) and interbursts (long, ~2 s). Bin sizes are 1 (left) and 400 (right) ms, respectively. ISI return map of burst I (***Cc***) represents one dense cluster with two arms, which corresponded to the interburst interval. ***Db***, Burst II contains four main rhythms, and ISI peaks are 12, 26, 39, and 50 ms. ***Dc***, ISI return map of burst II showing complex temporal features of the bursts.

(10.75 ± 1.60 Hz, 22 units) was significantly higher than the baseline activity before the operation (4.92 ± 0.73 Hz, 47 units). The spontaneous firing rate of the VPM units was slightly higher in the sham rats than in the IANx rats for the first few hours to the first day after surgery. However, the spontaneous activity of the VPM units in the sham group returned to baseline presurgery level 2 d after IANx and remained low until 60 d. This trend corresponds well with the behavior change in the sham rats (Fig. 1*B*).

Spontaneous firing patterns of TG and VPM units after IANx

Four types of ectopic firing patterns were observed in the resting wakeful condition after IANx: regular, slow irregular, and burst-like with or without a long interburst interval. Slow irregular firing was the dominant firing pattern of activated TG units after IANx (70% of the 10 activated TG V3 units, firing rate: 1.24 ± 0.84 Hz; 67% of the 9 activated TG V2 units; firing rate: 1.88 ± 1.02 Hz). Figure 5*Aa* shows the ISI distribution. One TG V2 unit (41.02 Hz) and one TG V3 unit (6.70 Hz) fired regularly (Fig. 5*B*). Two of the nine activated TG V2 units and 1 of the 10 activated TG V3 units had burst discharges interrupted by a long pause (0.25–2.2 s) (Fig. 5*Cb*, burst-I firing). As a burst developed, this type of unit displayed acceleration with a gradually decreasing ISI (inset of Fig. 5*Ca*). Another type of burst discharge fired in an integer multiple pattern (Fig. 5*D*, burst-II firing). Two TG V3 units fired in this manner, and their average firing rates were 22.9 and 67.2 Hz, respectively. A major peak of the ISI histogram of the former (Fig. 5*Db*) was 12 ms, and subsequent peaks appeared at 26, 38, and 50 ms. The pitch frequency of the latter unit was 4 ms, and subsequent peaks were 9, 13, 17, and 20 ms. Compared with the sham rats, the regular and the two types of burst firing patterns appeared only in the IANx rats.

Burst discharges in the ventroposterior lateral thalamic nucleus (VPL) are involved in the mechanisms of neuropathic pain following peripheral nerve injury (Lenz et al., 1998; Jhaveri et al., 2008). To test whether the burst-firing pattern became the dominant pattern in the VPM after IANx, the temporal firing patterns of VPM V2 units in conscious and isoflurane-anesthetized conditions were analyzed. In a conscious resting state, 96% of the VPM V2 units (44 of 46 units) fired in the tonic mode (5.05 ± 0.76 Hz) before the IANx/sham operation. Similarly, 80–94% of the VPM V2 units in the IANx (early: 25 of 31 units, 8.75 ± 1.96 Hz; late: 32 of 34 units, 8.81 ± 1.88 Hz) and sham-operated (early: 22 of 27 units, 7.49 ± 1.28 Hz; late: 20 of 25 units, 2.98 ± 0.61 Hz) rats also fired in the tonic mode (Fig. 6 *A–C*). The remaining units fired at a low frequency (<0.1 Hz). Thus, in the conscious resting state, the VPM thalamic units did not increase their bursting after IANx.

Under anesthesia, 53% of the VPM V2 units fired at a low frequency (25 of 47 units, 0.03 ± 0.01 Hz) before the IANx/sham operation. The remaining units were tonic (40%, 19 of 47 units) and bursty (6%, 3 of 47 units) (Fig. 6*D–I*). After IANx, a significantly higher percentage of the VPM V2 units began to fire in the burst mode during early (16%, 5 of 31 units, 0.16 ± 0.28 Hz) and late (18%, 6 of 34 units, 3.54 ± 3.15 Hz) phases of allodynia compared with preoperative condition ($p < 0.05$; Fig. 6*I*), reflecting a threefold increase in the number of burst firing units in the IANx condition. However, the predominant firing pattern of the VPM V2 units after IANx was still tonic firing during the early (61%, 19 of 31 units, 4.57 ± 1.34 Hz) and late (71%, 24 of 34

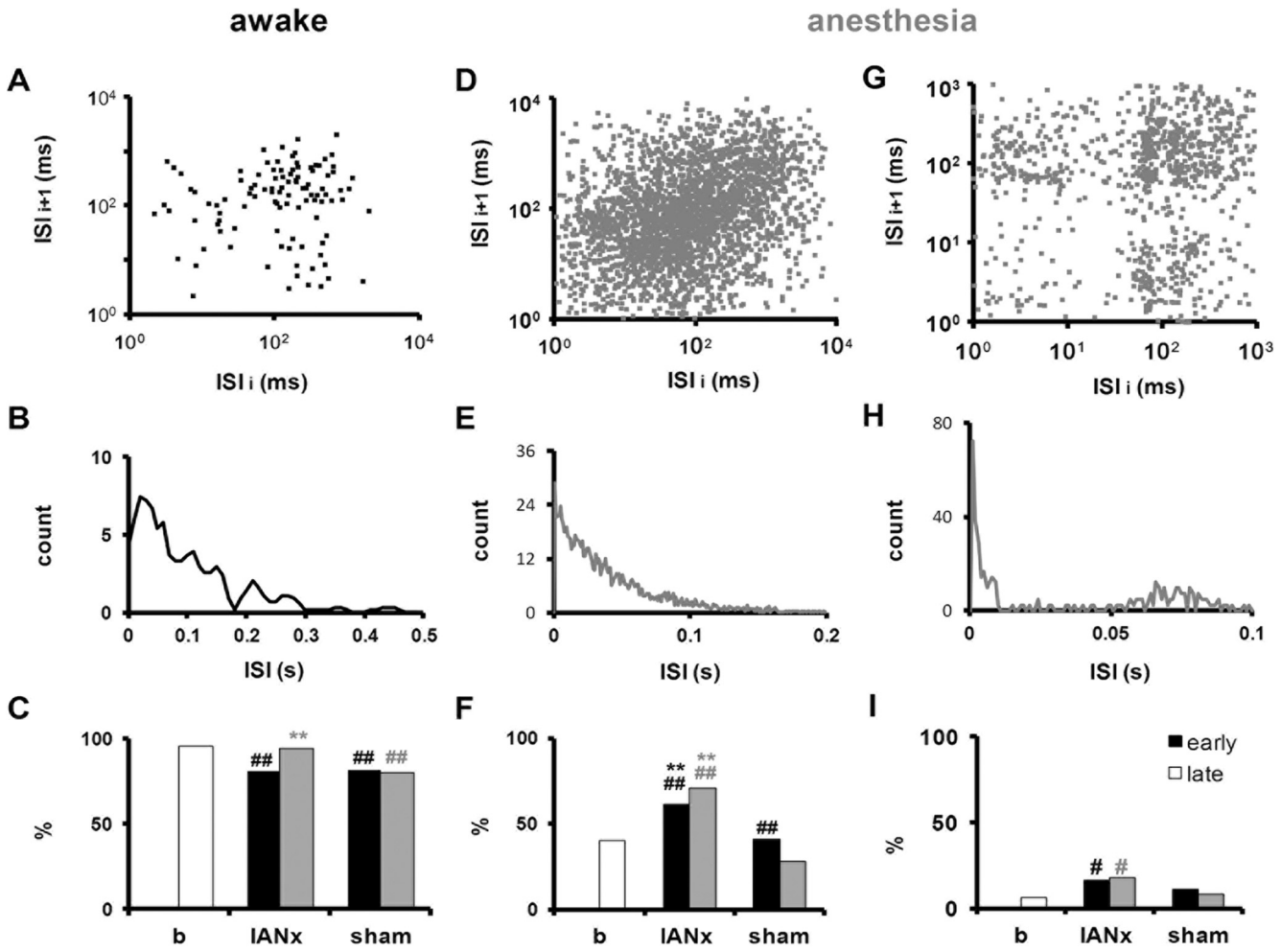

Figure 6. ***A***, ***B***, Tonic firing pattern in the VPM in wakeful IANx and control (i.e., sham-operated and the data before IANx/sham operation) rats. ***A***, ISI return map of a VPM V2 unit shows one dense cluster at the top right, which means equal pre- and post-ISIs and a tonic firing pattern. ***B***, ISI histogram of data in ***A***. ***C***, Percentage of VPM V2 units, which displayed a tonic firing pattern in IANx (46 units), sham-operated (46 units), and normal rats (before the operation, b; 47 units). Early (6 h to 3 d) and late (7–30 d) periods after operation are separated for analysis. The data before IANx and the sham operation were pooled in Group b. ***D–I***, Under anesthesia, tonic and burst VPM V2 units increased after IANx. ***D–F*** and ***G–I*** are respective examples of temporal patterns of tonic firing and bursting. ***D*** and ***G*** are ISI return maps. Note the four clusters in ***G***. The bottom right cluster mostly represents the first spikes in the burst. The bottom left cluster mostly represents spikes in the bursts, and the upper left cluster mostly indicates the last spikes in the burst. The upper right cluster mostly represents spikes in tonic mode. ***E*** and ***H*** are ISI histograms of data in ***D*** and ***G***. Percentages of tonic (***F***) and burst (***I***) VPM V2 units in normal, IANx, and sham-operated rats. Both firing types significantly increased after IANx. $^{\#}p < 0.05$, $^{\#\#}p < 0.01$ versus b (before IANx); $^{**}p < 0.01$, versus sham-operated rats according to a χ^2 test.

units, 2.16 ± 0.54 Hz) phases (Fig. 6*F*). The remaining units fired at a low frequency (<0.1 Hz).

Modulation of primary afferent and thalamic unit activities by anesthesia

Previous research on ferrets has shown that 0–26% of injured myelinated fibers exhibit spontaneous activity at 0.3–13 Hz from 3 to 113 d after IANx (Bongenhielm and Robinson, 1996). In the same neuropathic model (at 3 d), Tsuboi et al. (2004) demonstrated that 93% of V2 A fibers exhibited higher background activity (1–2 Hz) than those of naive rats. Consistent with these results, this study shows higher spontaneous activity in 23% of the TG units from the injured branch (6/26, mean spontaneous firing rate: 0.99 ± 0.22 Hz) and 26% of TG V2 units (5/19, mean spontaneous firing rate: 13.31 ± 4.03 Hz) in IANx rats under anesthesia. Spontaneous firing rate of TG units was significantly higher from 6 h to 30 d after transection (TG IAN: $p < 0.001$; TG V2: $p < 0.001$) than that of the sham-operated group (TG IAN: $n = 7$, 0.006 ± 0.004 Hz; TG V2: $n = 12$, 0.06 ± 0.02 Hz). The average firing rates of all TG units in the IAN and V2 division were 0.18 ± 0.02 Hz and 1.78 ± 0.63 Hz, respectively, and the spontaneous activities of both TG groups were significantly higher than those in the sham group (TG IAN: $p < 0.001$, $n = 7$; TG V2: $p < 0.05$, $n = 12$). This high spontaneous activity was detected within several hours and lasted until 30 d after IANx.

A corresponding increase of spontaneous activity under anesthetized condition also appeared in the VPM V2 neurons after IANx. The VPM V2 units exhibited significantly higher spontaneous activity (4.56 ± 1.51 Hz, 42 of 46 units) than the sham-operated group (0.46 ± 0.09 Hz, 36 of 46 units) from 6 h to 30 d after the transection ($p < 0.001$). This period of increased spontaneous activity was similar to that found in the TG V2 units. Figure 7 shows an analysis of the differences in TG and VPM spontaneous activities between conscious and anesthetized rats. Based on the assumption that general anesthesia suppresses neuronal activity, data points should be on the left side of the equality line (Figs. 7*C*,*F*, gray dotted lines). However, the data of the TG V2 units in the late phase (Fig. 7*C*, red line) shifted to the right side of the equality line, indicating that isoflurane anesthesia enhances spontaneous activity of the TG V2 units of IANx rats. The

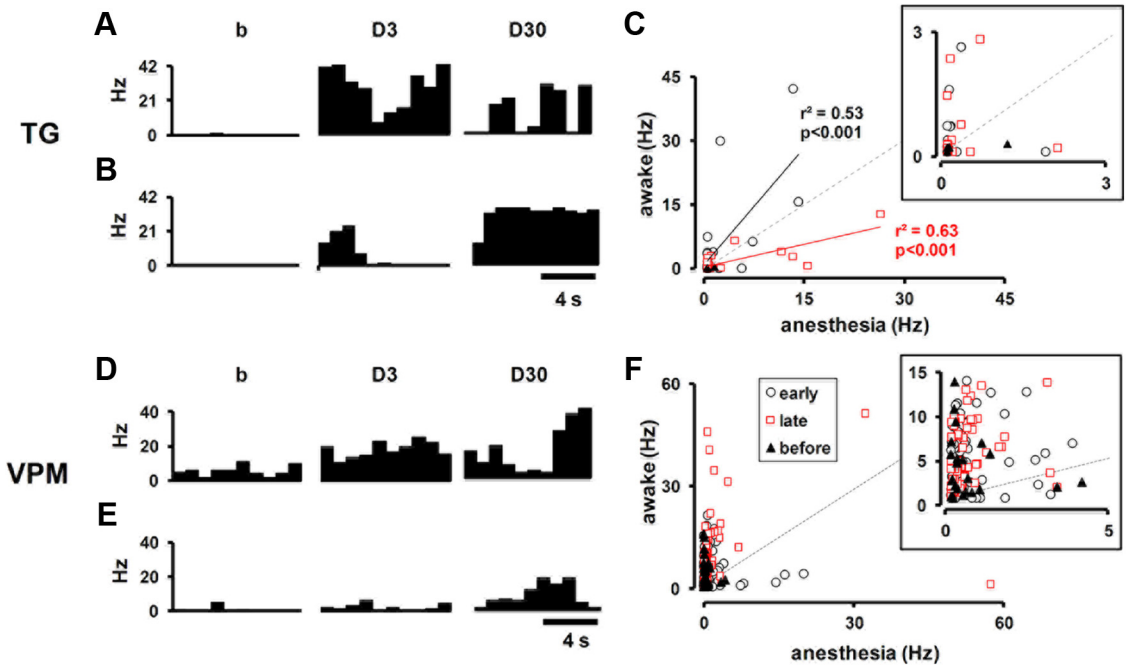

Figure 7. Differential anesthetic effect on spontaneous activities of TG V2 and VPM V2 units. ***A***, ***B***, Spontaneous activities of a TG V2 unit under awake (***A***) and anesthetic conditions (***B***) on the day before IANx and 3 and 30 d after IANx. During the early phase of allodynia (D3), isoflurane administration attenuated the spontaneous activity at 50 s from the beginning of the recording, whereas such suppression did not occur in the same unit during the late phase of allodynia (D30). ***C***, Distributions of spontaneous activity pairs in the anesthesia and awake conditions (from 19 TG V2 units). Each point represents the spontaneous activity of the same unit in both conditions. Data obtained from several days is separated into three groups: baseline (b; 5 units, 5 pairs), 6 h to 3 d after IANx (early; 10 units, 26 pairs), and 7–30 d after IANx (late; 10 units, 24 pairs). Correlation coefficients of early (red) and late (black) populations are shown. During the late phase of allodynia, isoflurane enhanced the spontaneous activity because the linear curve shifted to the right side of the gray dotted line, indicating a lack of anesthetic effects. ***D***, ***E***, Spontaneous activity of a VPM V2 unit in the awake (***D***) and anesthesia (***E***) conditions. All pairs of 46 VPM V2 units across days between awake and anesthetized conditions are plotted in ***F***. Isoflurane attenuated spontaneous activity of most of the VPM V2 unit during early-phase (31 units, 72 pairs) and late-phase (34 units, 78 pairs) allodynia and baseline firing frequency (25 units, 25 pairs). The correlation between both conditions disappeared ($r^2 < 0.1$). The bin size of the rate histogram was 1 s. Low firing-rate data in ***C*** and ***F*** are expanded and shown in insets.

effect of anesthetic drug was identified by subtracting the spontaneous activity under the anesthesia condition from that in the conscious condition. In the early phase of allodynia, isoflurane reduced the spontaneous activity of the TG V2 units (effect of anesthetic drug: -2.81 ± 1.50 Hz, 10 units). Conversely, isoflurane enhanced the spontaneous activity of the TG V2 units during the late phase of allodynia (effect of anesthetic drug: 1.38 ± 0.87 Hz, 10 units). The Wilcoxon signed-rank test ($p < 0.05$) showed a significant difference of the anesthesia effect between the two states. Four TG V2 units had isoflurane-enhanced responses to anesthesia after IANx during the late phase of allodynia (Figs. 7*A–C*). These units also exhibited a delay in attenuation by 1% isoflurane in the early phase (Fig. 7*B*, middle). Their spontaneous activity was high in the beginning of anesthesia, and terminated abruptly ~1 min later. During the late phase of allodynia, isoflurane administration did not decrease the activity of the TG V2 units, but enhanced it (Fig. 7*B*, right).

The Wilcoxon signed-rank test showed that the spontaneous activity of VPM V2 units was significantly attenuated by isoflurane in the baseline condition before IANx (-4.23 ± 0.98 Hz, $p < 0.001$, 25 units), early (-4.35 ± 0.77 Hz, $p < 0.001$, 31 units), and late (-6.90 ± 1.25 Hz, $p < 0.001$, 34 units) phases of allodynia (Fig. 7*D–F*). Some VPM V2 units showed enhanced spontaneous activity after isoflurane administration during the early (8 units) and late (1 unit) phases. Figure 7, *D* and *E*, show an exemplary effect of isoflurane on one VPM V2 unit.

Tactile-response change and RF size change under anesthesia

In addition to examining spontaneous activity changes, this study evaluates the responses to a series of mechanical stimuli in TG V2 and VPM V2 units under anesthesia. The tactile response (normalized to grand mean value of sham group) was significantly higher in the TG V2 units at 20–30 d after IANx (Fig. 8 *A–C*). The VPM V2 units showed stronger responses to tactile stimulation of the face 30 d after IANx (Fig. 8 *B*, *Cb*). In addition, one TG V2 unit and three VPM V2 units showed after-discharges following the cessation of the tactile stimulus in IANx rats (6–14 d). The duration of after-discharges ranged from 10 to 602 s after cessation of the tactile stimulus. In sham-operated rats, after-discharges were not apparent in the TG or VPM V2 units after tactile stimulation.

The RF size of each stable unit was measured chronically to determine whether it expands after IANx. After IANx, 10 stable VPM V2 units (nine pre-existing units and one new unit) significantly expanded their RFs in the late phase after IANx and returned to baseline (before IANx) at day 50 (Fig. 9*Ba*). However, the RF size of the TG V2 units and sham-operated groups did not change after IANx or sham operation (Fig. 9*Aa*,*Ab*,*Bb*).

Sensory modality shift of VPM units

Physiological and anatomical changes in myelinated fibers after nerve injury may induce allodynia (Latremoliere and Woolf, 2009; Devor, 2009a). This study tests whether tactile TG units or VPM units became pinch sensitive after IANx. Tactile TG V2 units did not change their modality after IANx (Fig. 10 *C*,*Ea*). However, tactile VPM V2 units became pinch sensitive at 6 h after nerve transection (average pinch response in the early phase, 3.04 ± 1.20 Hz, 11 of 31 units; Fig. 10*D*), and their responsiveness was significantly different from baseline ($p < 0.01$; Fig. 10*A*,*Da*). This modality change was apparent up to 30 d after IANx (late phase, 5.54 ± 3.67 Hz, 16 of 34 units; Fig. 10*D*).

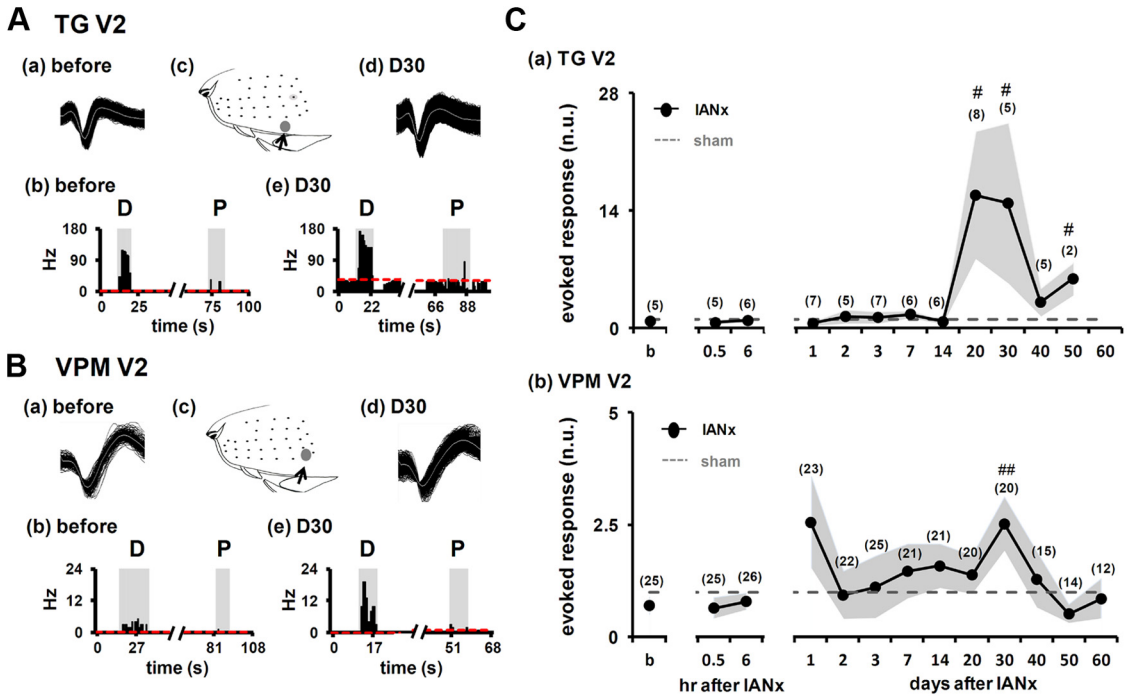

Figure 8. Increased evoked responses of TG and VPM V2 units to tactile mechanical stimulation after IANx. Examples from stable TG and VPM tactile units are shown in ***A*** and ***B***, respectively. Both low-threshold whisker units (the RF is indicated by an arrow in ***Ac*** and ***Bc***) in TG and VPM responded to deflection (D) stimulation of the whiskers, but not to pinch (P) stimulation. The gray shaded area denotes the stimulation period. A responsive criterion (red dotted line) is the mean + 2.33 SD of the 10 s baseline preceding each stimulation. At 30 d after IANx, evoked responses of TG and VPM units to tactile stimulation were enhanced (***Ae*** and ***Be***). Waveforms of units obtained from different time points are shown in ***a*** and ***d***. ***C***, Time-course changes in normalized evoked responses after IANx. The evoked response was normalized, divided by the mean value of the sham-operated group. The shaded area indicates the mean ± SEM. $^{\#}p < 0.05$, $^{\#\#}p < 0.01$, significantly differs from activity before IANx by the Mann–Whitney *U* test. Numerals in parentheses are the numbers of units.

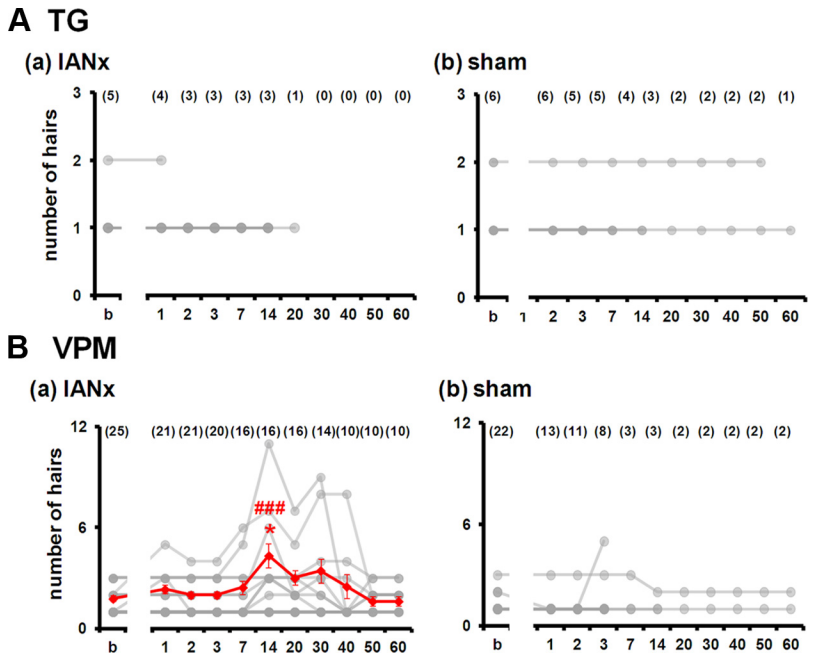

Figure 9. Expansion of RF size of VPM units after IANx. ***A***, Hair numbers of TG units in IANx (***Aa***) and sham-operated rats (***Ab***). The partially transparent gray dot denotes the number of hairs of each unit determined on a given day. ***B***, Number of hairs of VPM units significantly increased after IANx ($^{\#\#\#}p < 0.001$). The average value (red), calculated from 10 units with expanded RFs, is represented as the mean ± SEM. Numerals in parentheses are the unit numbers. $^{*}p < 0.05$ compared with sham group.

Conversely, in the sham-operated group, 19% of the VPM V2 units (5/27, 6.54 ± 3.90 Hz; Fig. 10*Db*) and 10% of the TG V2 units (1/10, 3.09 ± 3.09 Hz; Fig. 10*Eb*) also became pinch sensitive within 3 d of the operation. The mean value of pinch sensitivity in the TG V2 and VPM V2 units did not show a difference in the early and late phases after sham operation. A comparison of the percentage of modality-shifting units shows that the VPM V2 units in IANx rats had a significantly higher proportion of pinch-sensitive units than those in sham rats (Fig. 10*B*) during two phases of allodynia. There was no pinch-sensitive TG V2 unit in IANx rats during two phases, although one TG V2 unit became pinch sensitive in sham rats during the early phase (Fig. 10*C*). In addition, two VPM V2 modality-shifting units showed prolonged after-discharges after pinch stimulation in IANx rats (duration: 55 and 100 s, respectively).

Discussion

The immediate and long-term changes in the TG and VPM neuronal activities after IANx were longitudinally followed in chronically instrumented rats under conscious and anesthetized conditions. Figure 11 shows a summary of these new findings. The more important findings include the following: (1) specific burst and regular firing patterns in the IAN and V2 branches of the TG neurons after IANx; (2) a sequential increase in spontaneous activity from injured IAN ganglion neurons to uninjured V2 ganglion neurons, and then to VPM V2 neurons; and (3) RF expansion and modality shifting in the VPM V2 neurons after IANx.

Both IANx and sham-operated rats exhibited allodynia 1 d after surgery. The persistence of allodynia in IANx rats up to 30 d later indicates that differential mechanisms are involved in the IANx and sham-operated rats. The results in the present study show that the ectopic firing of the TG neurons but not the enhanced thalamic activity emerging after IANx distinguishes IANx from sham-operated rats in the development phase. On the other hand, in the late phase, the information transmitted by the sensitized and modality-shifted thalamic neurons may be misinterpreted as nociceptive, thereby maintaining allodynia.

Ectopic discharges of injured TG units

Ectopic discharges from injured ganglion neurons may be an initiator of neuropathic pain (Ochoa and Torebjörk, 1980; Nyström and Hagbarth, 1981; Baron, 2006). Based on the chronic recordings of TG and VPM neurons in conscious rats, this study confirms that ~30% of the injured TG neurons showed ectopic discharges after IANx. These ongoing activities can be classified as the following three patterns in sciatic nerve-injured rats: irregular, regular, or burst firing (Kajander et al., 1992; Amir et al., 1999, 2002; Sun et al., 2005). In this study, regular and burst firing patterns appeared only in IANx rats, in basic agreement with previous studies involving animals (Kajander et al., 1992; Amir et al., 1999, 2002; Sun et al., 2005) and patients (Ochoa and Torebjörk, 1980). The burst-I type (Fig. 5*C*) in this study is similar to the burst firing pattern reported in previous reports. Subthreshold membrane potential oscillations are involved in these burst firings in the primary afferent neurons following nerve injury, and maintained by postspike depolarizing after-potentials (Amir et al., 2002). In addition, previous research (Su et al., 2009) has shown firing patterns analogous to the burst-II patterns in this study (Fig. 5*D*). Pharmacological manipulations indicated the involvement of sodium channels in the generation of burst-II firing following IANx (Su et al., 2009).

In this study, the firing rate of the ectopic discharges in injured TG neurons ranged from 0.3 to 22 Hz, and 60% of these neurons fired at <1.5 Hz, which is slower than previously reported firing frequencies. For example, the spontaneous activity in peripheral nerve fibers was ~5 Hz following trigeminal nerve injury (Bongenhielm and Robinson, 1996; Kitagawa et al., 2006) and 15–40 Hz in the sciatic nerve following chronic constriction injury of the sciatic nerve (Kajander and Bennett, 1992; Devor, 2009a, b). The difference in firing frequency between previous research and this study most likely resulted from differences in experimental preparations. All previous reports were performed in acute experiments, mostly under anesthesia. The chronic recording method used in this study reduces injury discharges triggered by either microelectrode penetration or teased-fiber preparation. The ectopic discharges shown in previous studies may have been mixed with impulses generated by acute damage.

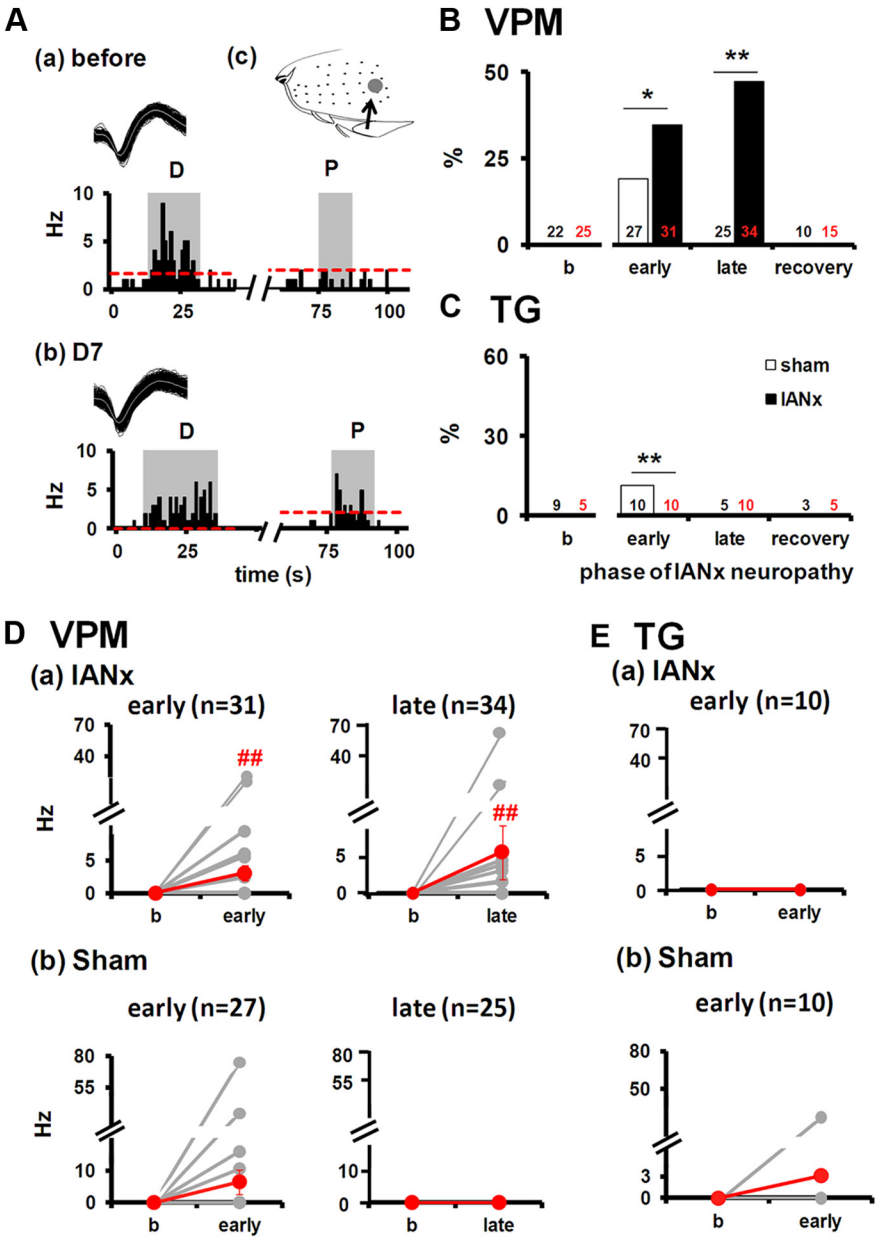

Figure 10. Modality shift of VPM V2 units after IANx. ***A***, Example from a stable whisker unit in the VPM before (***Aa***) and 7 d after IANx (***Ab***). This unit changed to be responsive to a pinch (P) of the skin over the RF (arrow in ***Ac***) after IANx. The gray shaded area in the histogram denotes the stimulation period. The red dotted line indicates the responsive criteria, evaluated by the mean + 2.33 SD of the 10 s baseline preceding each stimulation. D, Deflection of whiskers. The percentage of pinch-responsive units in the VPM (***B***) and TG (***C***) before IANx and during the early (6–3 d), late (730 d), and recovery (40–60 d) phases of neuropathic pain. Red and black numerals are unit numbers from IANx and sham-operated rats, respectively. A significant difference of pinch-responsive units with the sham group was evaluated by χ^2 or Fisher's exact test, respectively, indicated by $^{*}p < 0.05$ and $^{**}p < 0.01$. The average response amplitude to pinch stimulation in VPM V2 units was significantly enhanced after IANx (***Da***), whereas there was no difference in the sham-operated group (***Db***, ***Eb***) or in the group of TG V2 units (***Ea***). $^{\#\#}p < 0.01$, versus the baseline (the day before the IANx/sham operation) by the Wilcoxon signed-rank test.

Time-course difference between peripheral and central sensitization

Two hours after IANx, the TG V3 tactile units began to generate high-frequency spontaneous activity in conscious rats, and this

Figure 11. Summary schematic diagram of the possible underlying neural mechanism of allodynia in neuropathic pain (IANx vs sham-operated) and sham operation-induced pain (sham-operated vs the baseline) conditions. ***A***, In the neuropathic condition, the pathological process was separated into three phases: early, late, and recovery phases. During the early phase, injured A fibers (TG V3) produce burst-like or regular ectopic discharges followed by sensitization of adjacent uninjured A fibers (TG V2). These uninjured fibers transfer abnormal messages to the same division of the somatosensory thalamus (VPM V2), and trigger central sensitization in the late phase. These tactile VPM V2 neurons tend to have expanded RFs and tactile-evoked after-discharges, and tend to be sensitive to a pinch stimulus. Activation of these neurons by tactile stimulation may be mistaken as nociceptive information by the cortex and cause allodynia. In addition, when the pathological process is complete, anesthetics (or analgesic drugs) no longer reduce abnormal discharges. ***B***, Sham operation also produces transient extraterritorial allodynia, and only VPM V2 neurons display hyperexcitability. This shows that (1) cross talk in the CNS may produce extraterritorial allodynia of inflammation pain and (2) burst and regular spiking primary afferents are key injury messages to initiate the pathological process of neuropathy and strengthen central sensitization in the thalamus to maintain neuropathic pain.

period was earlier than VPM V2 units. The time-course differences in high-frequency spontaneous firing between TG V3, TG2, and VMP V2 confirm the notion that the tactile afferents from the injured nerve initiate pathological process associated with neuropathic pain (Kajander and Bennett, 1992; Kajander et al., 1992; Bongenhielm and Robinson, 1996; Tal et al., 1999; Yates et al., 2000; Sun et al., 2005).

The results in conscious animals with IANx showed that the barrage of action potentials in TG V2 units was generated within hours and lasted >30 d after IANx. The sensitization of TG V2 units is involved in the development of tactile allodynia (Tsuboi et al., 2004), and this hyperexcitability may be caused by abnormal voltage-gated potassium channels (Tsuboi et al., 2004; Takeda et al., 2011).

Recent research has shown that neuroplasticity changes occur in the cerebral cortex quickly (~3 h) after median nerve transection. These plastic changes may be caused by the disruption of safekeeping signal transduction through the low-frequency firing (0.1 Hz) of tactile fibers, resulting in the reorganization of the sensory map in humans (Tinazzi et al., 1997), primates (Jain et al., 2008), and rats (Barbay et al., 1999). Rapid thalamic sensitization within minutes after deafferentation (Garraghty and Kaas, 1991; Nicolelis et al., 1993; Jain et al., 2008; Kaas et al., 2008) may contribute to neuropathic pain initiation (Brüggemann et al.,

2001). This study shows that spontaneous activity of the VPM V2 neurons significantly increased 2 h after both IANx and sham operations. Initial timing of thalamic sensitization was similar to the injured IAN branch of the TG neurons. The enhancement of VPM V2 neuronal activity in sham-operated rats returned to baseline 1 d after the operation, whereas the hyperexcitability of VPM V2 neurons in IANx rats persisted until 30 d. Because the sham-operated rats exhibited higher thalamic activity than the IANx rats (Fig. 4*C*), it is unlikely that this period of thalamic hyperexcitation could initiate long-term extraterritorial allodynia. In human brain imaging research, skin and deep tissue incisions enhance sensory thalamic activity within hours (Pogatzki-Zahn et al., 2010). The early enhancement of VPM V2 activity after IANx and after sham operation may be due to tissue injury. It is still possible that, however, early thalamocortical sensitization may aid peripheral sensitization in initiating the development of neuropathic pain.

Modality shift of VPM V2 neurons as a cause of allodynia

Large diameter afferents undergo a change in their electrical characteristics and neurotransmitter expression following axotomy (Devor, 2009a). For example, after nerve injury, large diameter-injured fibers synthesize and release substance P (Noguchi et al., 1995; Malcangio et al., 2000; Pitcher and Henry, 2004; Weissner et al., 2006; Nitzan-Luques et al., 2011) and calcitonin gene-related peptide (CGRP) (Ma and Bisby, 1998; Ma et al., 2003), which is normally only expressed in the small diameter unmyelinated fibers. Increased CGRP and substance P expression in the gracile nucleus, which receives most inputs from large diameter dorsal root ganglion neurons, appear after sciatic nerve injury (Noguchi et al., 1995; Ma et al., 1999; Nitzan-Luques et al., 2011). These results suggest that the phenotype switch of these tactile neurons may contribute to spontaneous pain and tactile allodynia (Nitzan-Luques et al., 2011).

Results show that 35 and 47% of the VPM V2 units became sensitive to pinch stimulation in the early and late phases after IANx, respectively, whereas no TG V2 tactile units became pinch sensitive after IANx. The *de novo* expression and release of neuropeptides in the primary tactile neurons may possibly affect postsynaptic neurons, rather than the modality of presynaptic tactile neurons. In the thalamus, the modality shift occurred in VPL neurons from a low threshold to a high threshold within 1–2 h after partial ligation of the sciatic nerve (Brüggemann et al., 2001). Because this study does not test the mechanical evoked responses under anesthesia from 1 to 5 h, we cannot determine the onset of the modality shift in the VPM after IANx.

In conclusion, the hyperexcitability of injured IAN TG neurons may initiate the sensitization of uninjured TG neurons. This in turn generates high-frequency firing in thalamic neurons, contributing to neuroplastic changes in the thalamocortical circuits, and producing long-lasting neuropathic pain in the orofacial region.

References

Adrian ED (1930) The effects of injury on mammalian nerve fibres. Proc Roy Soc Ser B 106:596–618. CrossRef

Amir R, Michaelis M, Devor M (1999) Membrane potential oscillations in dorsal root ganglion neurons: role in normal electrogenesis and neuropathic pain. J Neurosci 19:8589–8596. Medline

Amir R, Michaelis M, Devor M (2002) Burst discharge in primary sensory neurons: triggered by subthreshold oscillations, maintained by depolarizing afterpotentials. J Neurosci 22:1187–1198. Medline

Barbay S, Peden EK, Falchook G, Nudo RJ (1999) Sensitivity of neurons in somatosensory cortex (S1) to cutaneous stimulation of the hindlimb immediately following a sciatic nerve crush. Somatosens Mot Res 16:103–114. CrossRef Medline

Baron R (2006) Mechanisms of disease: neuropathic pain—a clinical perspective. Nat Clin Pract Neurol 2:95–106. CrossRef Medline

Bongenhielm U, Robinson PP (1996) Spontaneous and mechanically evoked afferent activity originating from myelinated fibres in ferret inferior alveolar nerve neuromas. Pain 67:399–406. CrossRef Medline

Brüggemann J, Galhardo V, Apkarian AV (2001) Immediate reorganization of the rat somatosensory thalamus after partial ligation of sciatic nerve. J Pain 2:220–228. CrossRef Medline

Campbell JN, Meyer RA (2006) Mechanisms of neuropathic pain. Neuron 52:77–92. CrossRef Medline

Chung JM, Leem JW, Kim SH (1992) Somatic afferent fibers which continuously discharge after being isolated from their receptors. Brain Res 599:29–33. CrossRef Medline

Costigan M, Scholz J, Woolf CJ (2009) Neuropathic pain: a maladaptive response of the nervous system to damage. Annu Rev Neurosci 32:1–32. CrossRef Medline

Davis KD, Taylor KS, Anastakis DJ (2011) Nerve injury triggers changes in the brain. Neuroscientist 17:407–422. CrossRef Medline

Devor M (2009a) Ectopic discharge in A beta afferents as a source of neuropathic pain. Exp Brain Res 196:115–128. CrossRef Medline

Devor M (2009b) Ectopia generators. In: Science of pain (Basbaum AI, Bushnell MC, eds), pp 83–88. San Diego: Academic.

Fischer TZ, Tan AM, Waxman SG (2009) Thalamic neuron hyperexcitability and enlarged receptive fields in the STZ model of diabetic pain. Brain Res 1268:154–161. CrossRef Medline

Fried K, Bongenhielm U, Boissonade FM, Robinson PP (2001) Nerve injury-induced pain in the trigeminal system. Neuroscientist 7:155–165. CrossRef Medline

Garraghty PE, Kaas JH (1991) Functional reorganization in adult monkey thalamus after peripheral nerve injury. Neuroreport 2:747–750. CrossRef Medline

Hains BC, Saab CY, Waxman SG (2006) Alterations in burst firing of thalamic VPL neurons and reversal by Na(v)1.3 antisense after spinal cord injury. J Neurophysiol 95:3343–3352. CrossRef Medline

Iwata K, Imai T, Tsuboi Y, Tashiro A, Ogawa A, Morimoto T, Masuda Y, Tachibana Y, Hu J (2001) Alteration of medullary dorsal horn neuronal activity following inferior alveolar nerve transection in rats. J Neurophysiol 86:2868–2877. Medline

Iwata K, Tsuboi Y, Shima A, Harada T, Ren K, Kanda K, Kitagawa J (2004) Central neuronal changes after nerve injury: neuroplastic influences of injury and aging. J Orofac Pain 18:293–298. Medline

Jain N, Qi HX, Collins CE, Kaas JH (2008) Large-scale reorganization in the somatosensory cortex and thalamus after sensory loss in macaque monkeys. J Neurosci 28:11042–11060. CrossRef Medline

Jhaveri MD, Elmes SJ, Richardson D, Barrett DA, Kendall DA, Mason R, Chapman V (2008) Evidence for a novel functional role of cannabinoid CB(2) receptors in the thalamus of neuropathic rats. Eur J Neurosci 27:1722–1730. CrossRef Medline

Ji RR, Strichartz G (2004) Cell signaling and the genesis of neuropathic pain. Sci STKE 2004:reE14. Medline

Kaas JH, Qi HX, Burish MJ, Gharbawie OA, Onifer SM, Massey JM (2008) Cortical and subcortical plasticity in the brains of humans, primates, and rats after damage to sensory afferents in the dorsal columns of the spinal cord. Exp Neurol 209:407–416. CrossRef Medline

Kajander KC, Bennett GJ (1992) Onset of a painful peripheral neuropathy in rat: a partial and differential deafferentation and spontaneous discharge in A beta and A delta primary afferent neurons. J Neurophysiol 68:734–744. Medline

Kajander KC, Wakisaka S, Bennett GJ (1992) Spontaneous discharge originates in the dorsal root ganglion at the onset of a painful peripheral neuropathy in the rat. Neurosci Lett 138:225–228. CrossRef Medline

Kitagawa J, Takeda M, Suzuki I, Kadoi J, Tsuboi Y, Honda K, Matsumoto S, Nakagawa H, Tanabe A, Iwata K (2006) Mechanisms involved in modulation of trigeminal primary afferent activity in rats with peripheral mononeuropathy. Eur J Neurosci 24:1976–1986. CrossRef Medline

Komagata S, Chen S, Suzuki A, Yamashita H, Hishida R, Maeda T, Shibata M, Shibuki K (2011) Initial phase of neuropathic pain within a few hours after nerve injury in mice. J Neurosci 31:4896–4905. CrossRef Medline

Kubota I, Tsuboi Y, Shoda E, Kondo M, Masuda Y, Kitagawa J, Oi Y, Iwata K (2007) Modulation of neuronal activity in CNS pain pathways following

propofol administration in rats: Fos and EEG analysis. Exp Brain Res 179:181–190. CrossRef Medline

Latremoliere A, Woolf CJ (2009) Central sensitization: a generator of pain hypersensitivity by central neural plasticity. J Pain 10:895–926. CrossRef Medline

Lenz FA, Kwan HC, Dostrovsky JO, Tasker RR (1989) Characteristics of the bursting pattern of action potentials that occurs in the thalamus of patients with central pain. Brain Res 496:357–360. CrossRef Medline

Lenz FA, Kwan HC, Martin R, Tasker R, Richardson RT, Dostrovsky JO (1994) Characteristics of somatotopic organization and spontaneous neuronal activity in the region of the thalamic principal sensory nucleus in patients with spinal cord transection. J Neurophysiol 72:1570–1587. Medline

Lenz FA, Garonzik IM, Zirh TA, Dougherty PM (1998) Neuronal activity in the region of the thalamic principal sensory nucleus (ventralis caudalis) in patients with pain following amputations. Neuroscience 86:1065–1081. CrossRef Medline

Ma W, Bisby MA (1998) Increase of calcitonin gene-related peptide immunoreactivity in the axonal fibers of the gracile nuclei of adult and aged rats after complete and partial sciatic nerve injuries. Exp Neurol 152:137–149. CrossRef Medline

Ma W, Ramer MS, Bisby MA (1999) Increased calcitonin gene-related peptide immunoreactivity in gracile nucleus after partial sciatic nerve injury: age-dependent and originating from spared sensory neurons. Exp Neurol 159:459–473. CrossRef Medline

Ma W, Chabot JG, Powell KJ, Jhamandas K, Dickerson IM, Quirion R (2003) Localization and modulation of calcitonin gene-related peptide-receptor component protein-immunoreactive cells in the rat central and peripheral nervous systems. Neuroscience 120:677–694. CrossRef Medline

Macefield VG (1998) Spontaneous and evoked ectopic discharges recorded from single human axons. Muscle Nerve 21:461–468. CrossRef Medline

Malcangio M, Ramer MS, Jones MG, McMahon SB (2000) Abnormal substance P release from the spinal cord following injury to primary sensory neurons. Eur J Neurosci 12:397–399. CrossRef Medline

Nicolelis MA, Lin RC, Woodward DJ, Chapin JK (1993) Induction of immediate spatiotemporal changes in thalamic networks by peripheral block of ascending cutaneous information. Nature 361:533–536. CrossRef Medline

Nitzan-Luques A, Devor M, Tal M (2011) Genotype-selective phenotypic switch in primary afferent neurons contributes to neuropathic pain. Pain 152:2413–2426. CrossRef Medline

Noguchi K, Kawai Y, Fukuoka T, Senba E, Miki K (1995) Substance P induced by peripheral nerve injury in primary afferent sensory neurons and its effect on dorsal column nucleus neurons. J Neurosci 15:7633–7643. Medline

Nyström B, Hagbarth KE (1981) Microelectrode recordings from transected nerves in amputees with phantom limb pain. Neurosci Lett 27:211–216. CrossRef Medline

Ochoa JL, Torebjörk HE (1980) Paraesthesiae from ectopic impulse generation in human sensory nerves. Brain 103:835–853. CrossRef Medline

Pitcher GM, Henry JL (2004) Nociceptive response to innocuous mechanical stimulation is mediated via myelinated afferents and NK-1 receptor activation in a rat model of neuropathic pain. Exp Neurol 186:173–197. CrossRef Medline

Pogatzki-Zahn EM, Wagner C, Meinhardt-Renner A, Burgmer M, Beste C, Zahn PK, Pfleiderer B (2010) Coding of incisional pain in the brain: a functional magnetic resonance imaging study in human volunteers. Anesthesiology 112:406–417. CrossRef Medline

Seltzer Z, Beilin BZ, Ginzburg R, Paran Y, Shimko T (1991) The role of injury discharge in the induction of neuropathic pain behavior in rats. Pain 46:327–336. CrossRef Medline

Shoda E, Kitagawa J, Suzuki I, Nitta-Kubota I, Miyamoto M, Tsuboi Y, Kondo M, Masuda Y, Oi Y, Ren K, Iwata K (2009) Increased phosphorylation of extracellular signal-regulated kinase in trigeminal nociceptive neurons following propofol administration in rats. J Pain 10:573–585. CrossRef Medline

Su X, Liang AH, Urban MO (2009) The effect of amitriptyline on ectopic discharge of primary afferent fibers in the L5 dorsal root in a rat model of neuropathic pain. Anesth Analg 108:1671–1679. CrossRef Medline

Sun Q, Tu H, Xing GG, Han JS, Wan Y (2005) Ectopic discharges from injured nerve fibers are highly correlated with tactile allodynia only in early, but not late, stage in rats with spinal nerve ligation. Exp Neurol 191:128–136. CrossRef Medline

Takeda M, Tsuboi Y, Kitagawa J, Nakagawa K, Iwata K, Matsumoto S (2011) Potassium channels as a potential therapeutic target for trigeminal neuropathic and inflammatory pain. Mol Pain 7.

Tal M, Wall PD, Devor M (1999) Myelinated afferent fiber types that become spontaneously active and mechanosensitive following nerve transection in the rat. Brain Res 824:218–223. CrossRef Medline

Tinazzi M, Zanette G, Polo A, Volpato D, Manganotti P, Bonato C, Testoni R, Fiaschi A (1997) Transient deafferentation in humans induces rapid modulation of primary sensory cortex not associated with subcortical changes: a somatosensory evoked potential study. Neurosci Lett 223: 21–24. CrossRef Medline

Tseng WT, Yen CT, Tsai ML (2011) A bundled microwire array for long-term chronic single-unit recording in deep brain regions of behaving rats. J Neurosci Methods 201:368–376. CrossRef Medline

Tsuboi Y, Takeda M, Tanimoto T, Ikeda M, Matsumoto S, Kitagawa J, Teramoto K, Simizu K, Yamazaki Y, Shima A, Ren K, Iwata K (2004) Alteration of the second branch of the trigeminal nerve activity following inferior alveolar nerve transection in rats. Pain 111:323–334. CrossRef Medline

Vos BP, Benoist JM, Gautron M, Guilbaud G (2000) Changes in neuronal activities in the two ventral posterior medial thalamic nuclei in an experimental model of trigeminal pain in the rat by constriction of one infraorbital nerve. Somatosens Mot Res 17:109–122. CrossRef Medline

Wall PD, Waxman S, Basbaum AI (1974) Ongoing activity in peripheral nerve: injury discharge. Exp Neurol 45:576–589. CrossRef Medline

Weissner W, Winterson BJ, Stuart-Tilley A, Devor M, Bove GM (2006) Time course of substance P expression in dorsal root ganglia following complete spinal nerve transection. J Comp Neurol 497:78–87. CrossRef Medline

Woolf CJ, Mannion RJ (1999) Neuropathic pain: aetiology, symptoms, mechanisms, and management. Lancet 353:1959–1964. CrossRef Medline

Yates JM, Smith KG, Robinson PP (2000) Ectopic neural activity from myelinated afferent fibres in the lingual nerve of the ferret following three types of injury. Brain Res 874:37–47. CrossRef Medline

Zimmermann M (1983) Ethical guidelines for investigations of experimental pain in conscious animals. Pain 16:109–110. CrossRef Medline